2018

Modeling A Scroll Compressor Using A Cartesian Cut-Cell Based CFD Methodology With Automatic Adaptive Meshing

Ha-Duong Pham
Sanden International Europe (Ltd), German Branch, h.pham@sanden-europe.com

Thomas Brandt
Sanden International Europe (Ltd), German Branch, t.brandt@sanden-europe.com

David Henry Rowinski
Convergent Science, Inc., United States of America, david.rowinski@convergecfd.com

Modeling a Scroll Compressor Using a Cartesian Cut-Cell Based CFD Methodology with Automatic Adaptive Meshing

David ROWINSKI[1*], Ha-Duong PHAM[2], Thomas BRANDT[2]

[1]Convergent Science, Inc.,
Madison, WI, USA
david.rowinski@convergecfd.com

[2]Sanden International Europe (Ltd), German Branch,
Bad Nauheim, Germany
h.pham@sanden-europe.com
t.brandt@sanden-europe.com

* Corresponding Author

ABSTRACT

The recent requirements on the scroll compressors used in air conditioning systems are focused on the reduction of the noise and the improvement of the efficiency. To achieve this, the complex fluid flow phenomenon taking place inside of the compressor must be better understood. Two modeling approaches for investigating this problem are one-dimensional multi-physics modeling and three-dimensional computational fluid dynamics (CFD) modeling. The one-dimensional multi-physics based models are available to perform these calculations with low computational cost, but the influence of detailed geometrical effects on the fluid flow behavior is not taken into account.

This paper deals with the development and application of a three-dimensional CFD model for a scroll compressor. To deal with the challenge of the complicated moving geometries of the orbiting scroll and the deforming reed valves, an automated meshing strategy is employed to dynamically calculate the working chamber volumes based on the instantaneous geometry positions. Thereby no user meshing is required, and the resulting Cartesian cut-cell based mesh has the desirable numerical properties of orthogonality and low numerical diffusion. The motion of the discharge reed valve is determined using a fluid-structure-interaction model considering the valve as a one-dimensional deforming cantilever beam and considering the valve geometry and variable cross sections. The comparisons between the simulation and experimental results, e.g. indicator diagram, discharge valve motion and deformation, and pressure pulsation indicate that a good correlation is achieved, while the computational time stays acceptably low. The spatial and temporal convergence of the numerical method is demonstrated, particularly for the computation of the internal pressure and discharge pressure pulsation. The results show that the developed simulation model can be used to improve and to optimize the compressor design process by reducing the demand on prototype testing and to improve the understanding of the internal flow in the system.

1. INTRODUCTION

In order to have a good compressor design with high efficiency and low noise level for electric vehicles, a detailed understanding about the complex fluid flow inside the compressor is a crucial requirement. Furthermore, regarding the design optimization phase, the influence of the geometry changes on the compressor efficiency and pulsation level must also be clarified. To deal with these challenging issues, two modeling approaches, namely 1D multi-physics and 3D CFD simulation, can be used.

The 1D multi-physics simulations in general can offer quite accurate results as compared to the measurement with low computation time, for example 15 minutes for three operating conditions as reported by Pham (2016). The primary limitation of this approach, however, is that the influence of the 3D geometry changes, for example the effects of the muffler on the pressure pulsation, cannot be considered. In addition to this, the working chamber

volumes and the opening angle of the discharge valve as function of the orbiting angle must be pre-calculated and treated as input parameters. Finite element modeling (FEM) analysis has to be carried out before hand to predict the mass equivalence and stiffness for the valve modeling. This limits the flexibility and applicability of the 1D modeling methods.

The 3D CFD simulation combined with fluid structure interaction (FSI) can provide better accuracy compared to the 1D approach because the 3D geometry effect is directly considered. This is suitable for the optimization phase of design. Several investigations regarding 3D CFD simulation applied to scroll compressors were presented, including the studies of Gao (2014) and Xiao (2014), as well as the studies of Hesse (2016) in a dry scroll vacuum pump and Picavet (2016) in a refrigeration scroll compressor with a discharge valve. All of these investigation used the moving mesh technique to model the motion of the orbiting scroll and the valve motion, which leads to a high computation time. The obtained results show the feasibility of the 3D CFD model applied to scroll compressors, but there is considerable room for improvements in terms of the accuracy and the computational time for optimization in engineering design applications.

The current work presents an alternate CFD approach based on the cut-cell method for this type of problem. The key advantages of this method are: (1) little setup time required to go from a CAD geometry to a CFD model; (2) parametric changes to the design geometry can easily be incorporated into the model or entirely automated; (3) a stationary mesh with orthogonal cells has high numerical accuracy and stability and no numerical diffusion otherwise associated with moving mesh approaches; (4) a modified cut-cell based geometrical reconstruction of the cells at moving boundaries permits general motion of any boundary (including the orbiting scrolls and the discharge reed valves) while conserving mass, momentum, energy, and species; (5) the use of adaptive mesh refinement allows dynamic allocation of high resolution cells to times and locations where the gradients of flow variables are highest. This work will for the first time present this CFD method in the context of a scroll compressor with a reed valve, validate the model against experimental data, and demonstrate the cost and accuracy for different grid refinement levels.

2. EXPERIMENTAL METHODOLOGY

The validation of the simulation result was carried out using a Sanden scroll compressor, which is used for the air conditioning (AC) system in the automobile industry. Figure 1 shows the test apparatus for the measurement of the pressure inside the working chambers and the valve lift. The pressure sensors are directly mounted on the compressor rear casing, and a total of six sensors were positioned to record the compression process for each of the two sides of the scroll interior, so a total of three sensors with a small amount of overlap was required to determine the compression curve. The discharge reed valve lift was measured with both a strain gauge mounted on the reed and an eddy current sensor mounted on the valve retainer, also shown in Figure 1.

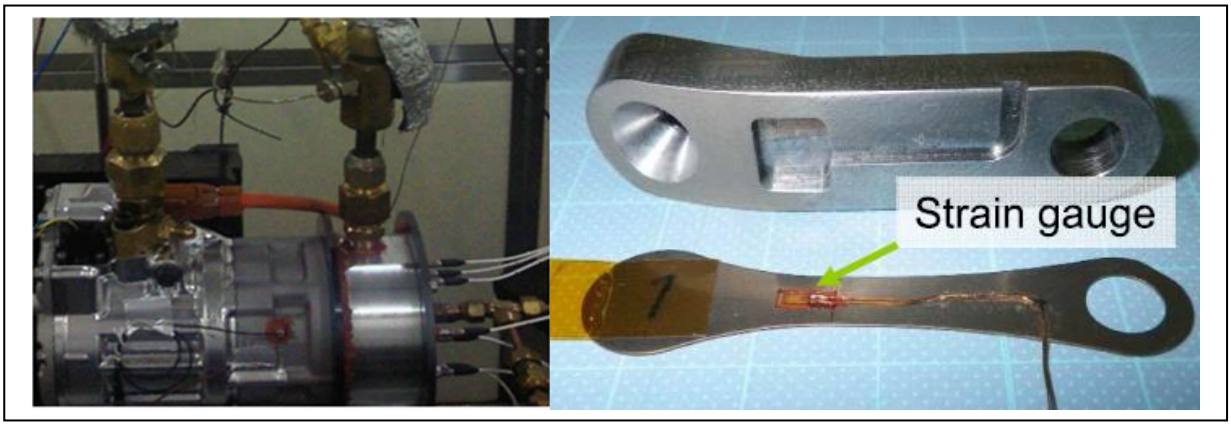

Figure 1: Testing apparatus for measurement of the internal chamber pressures, i.e. the indicator diagram. To the right is the discharge reed valve and retainer along with the strain gauge used for lift measurement. The eddy current sensor sits in the recess of the retainer.

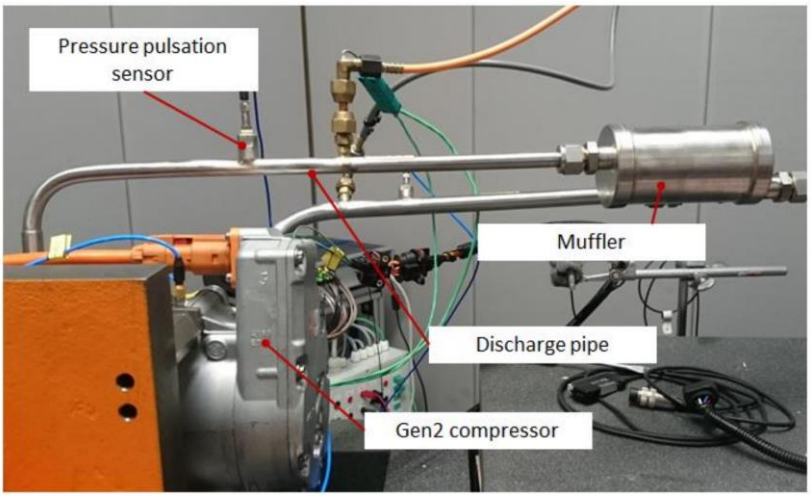

Figure 2: Photograph of the experimental testing apparatus for measuring the discharge pressure pulsation.

Figure 2 depicts the test bench used to measure the pressure pulsation. The sensor was a PCB Pieozotronics model 112A21, capable of measuring both static and dynamic pressures. The sensor was positioned in front of the hot gas silencer. The compressor used R-134a as the working fluid and operated at a suction pressure of 3 bar (absolute) for all operating conditions studied in this work. The discharge pressure ranged from 15 bar to 26 bar (absolute), and the shaft speed varied from 1000 rpm to 8500 rpm.

3. NUMERICAL MODELS

The CAD assembly of the compressor components was merged together to form an enclosed path of the working fluid. This was then exported into a triangulated surface, shown in Figure 3, which serves as the geometry input for the CFD solver. The flow enters the suction muffler (3.1), flows through the passages of the fixed scroll (3.2) and orbiting scroll (3.3), exits the discharge port (3.4) by opening the reed valve (3.5), flows into the suction muffler (3.6), through the discharge orifice (3.7), and finally through the discharge pipe (3.8).

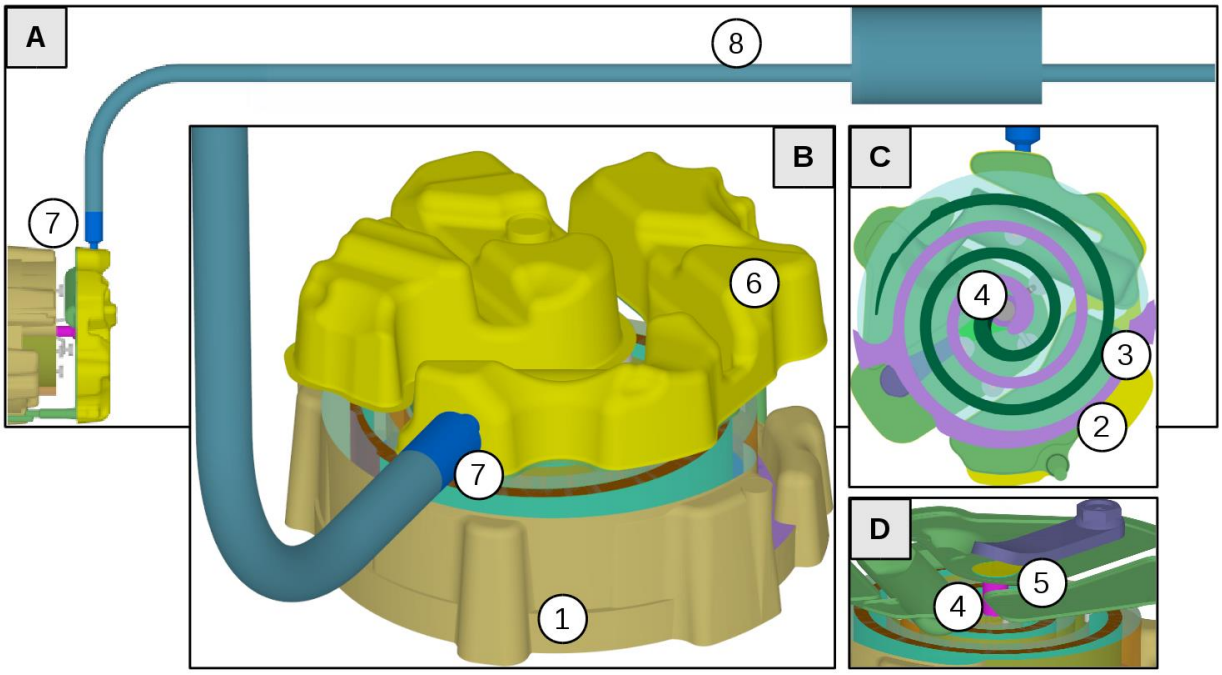

Figure 3: Computational domain extracted from the CAD geometry. In (A) is the discharge pipe, (B) shows the discharge muffler, (C) shows the orbiting and fixed scrolls, and (D) shows the detail of the discharge port and valve.

3.1 Flow Solver

The CFD solver automatically constructs the mesh at run time using the cut-cell based approach described by Senecal (2007) and Richards (2017) and available in the commercially available software package CONVERGE. Orthogonal Cartesian cells are populated in the interior at a user-specified size, the base grid size. At the boundaries, where the triangulated surface intersects with the cells, the cells are cut by the bounding surface into polyhedral. Even though these polyhedral are cut, they still retain the geometry volume. As the surfaces move independently, the boundary cells get cut and re-formed at every time step, and the appropriate boundary fluxes enter each cell to maintain consistency with the governing modeled equations. The method of adaptive mesh refinement, as used by Pomraning (2014), adds mesh resolution based on gradients of flow variables.

The governing equations for mass, momentum, energy, and equation of state are solved to determine the pressure, velocity, density, and temperature throughout the mesh. Values are solved for and stored collocated at the cell centers. The scheme of Rhie (1983) is used to prevent checker-boarding on the collocated grid. Pressure-velocity coupling is accomplished through the pressure implicit with splitting of operators (PISO) method of Issa (1985). All equations are solved with second order accuracy in space and first order fully implicit in time for stability. The RNG k-epsilon turbulence model of Yakhot (1986) is also used to account for effects of turbulence. This requires the solution of two extra modeled equations, the turbulent kinetic energy and the turbulence dissipation rate. The equation of state and all thermodynamic (specific heat, internal energy, enthalpy) and transport properties (molecular viscosity and conductivity) for R-134a are computed from structured look-up tables calculated using the software library of Bell (2014) and the properties from Tillner-Roth (1994).

3.3 Solid Solver and Coupling

The deformation of the reed valve is a crucial part of the simulation, and is easy to incorporate given the cut-cell method's ability to handle moving geometries. The reed is discretized along its length and treated as a one-dimensional Euler beam as in Rowinski (2016). At each node, the stress and strain is computed and the beam deforms. The pressure is computed from the local fluid pressure at each node. The same penalty force contact method as in Rowinski (2016) is used to handle contact with the retainer and seat. The domains are coupled in an explicit manner; the fluid is solved at a single time step, and then transfers the pressure loads to the solid solver, which then evaluates the solid solution and moves the beam nodes, and the fluid solver proceeds with the next step.

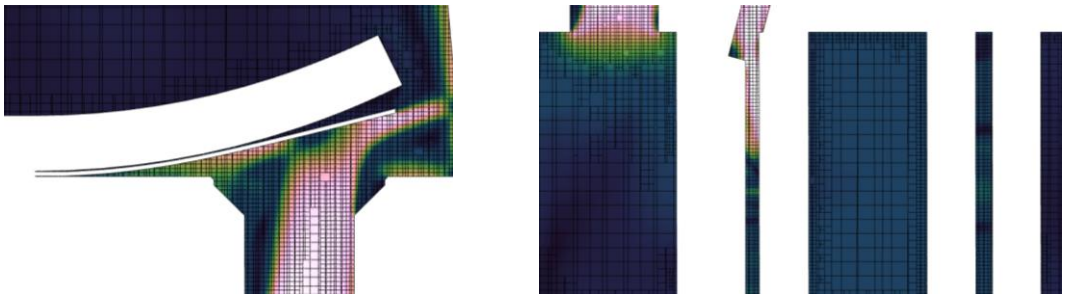

Figure 4: Reed valve model through deforming Euler beam (left) and full geometric axial seals (right)

3.3 Sealing

Since the physical geometry features oil lubricated tip seals at the axial ends of the orbiting scroll, a numerical sealing method is also applied at the axial ends of the orbiting scroll to totally cut off the flow in this direction. These seals project the orbiting scroll onto the fixed wall and re-compute the surface triangulation at each time step. Where the ports open or pressure transducer channels appear, an intersecting seal forms the union of the joined parts to allow a partial flow passage as determined by the blockage.

4. RESULTS

To compute the steady state condition, the base cases are run until the discharge pressure and compression pressures reach cyclic convergence, which typically was around five revolutions of the orbiting scroll. From this condition, simulations were conducted for an additional five revolutions on finer grids. A total of seven operating conditions were examined including speeds of 3000, 5000, and 7000 rpm, and discharge pressures of 15, 21, and 26 bar.

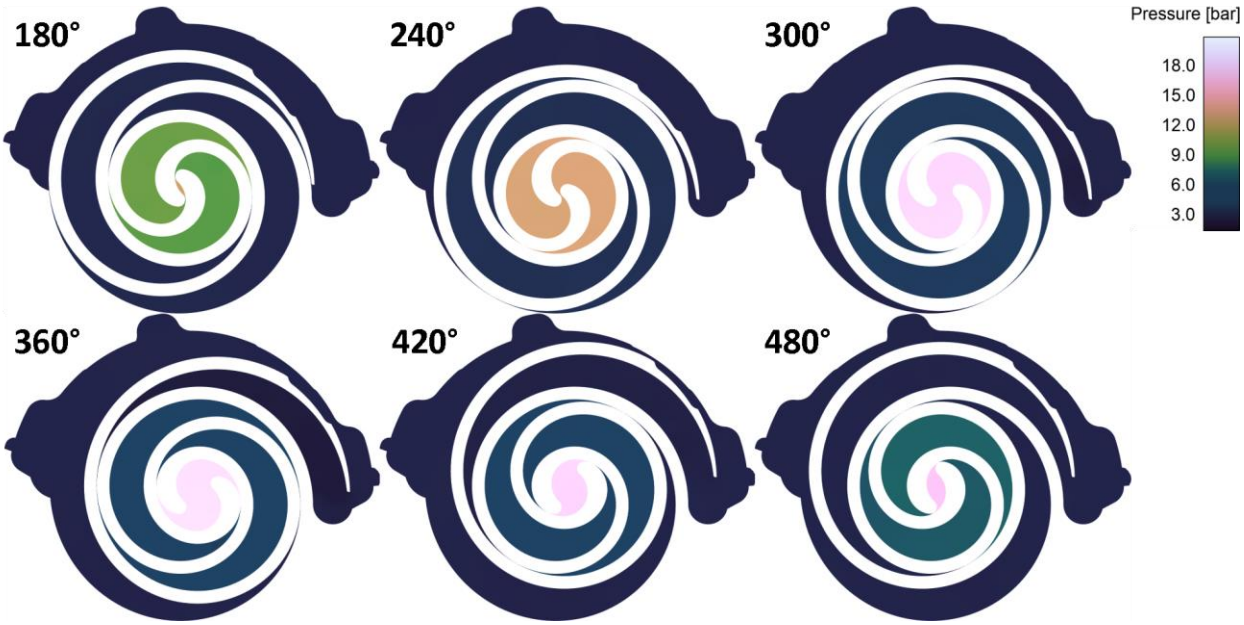

Figure 5: Planes down the center of the compression chambers colored by pressure.

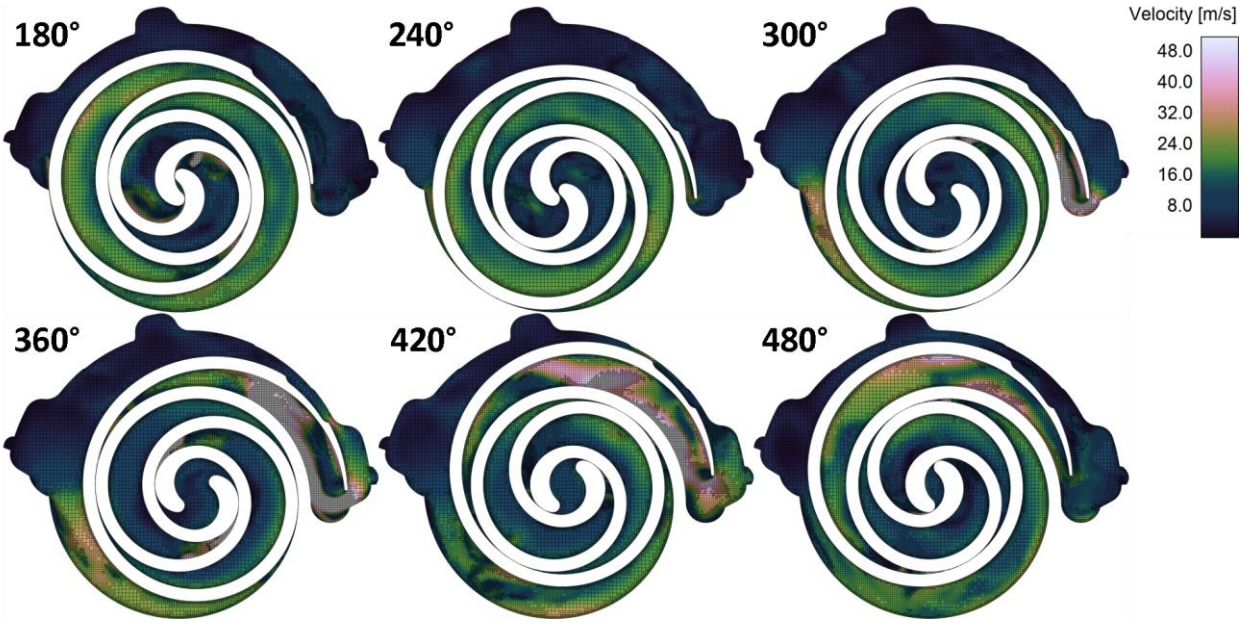

Figure 6: Planes along the center of the compression chambers with the grid overlaid and colored by velocity.

4.1 Base Case Results

Figures 5 and 6 show some typical results of the 7000 rpm, 15 bar discharge pressure cases, including the chamber pressures in Figure 5, and the internal velocities in Figure 6. From these figures, it can be seen that the total compression process for each chamber requires approximately three rotations of the orbiting scroll. The compression process starts at 180 degrees, where the volume is first trapped after suction. It is then compressed as the scrolls wrap until it reaches a high pressure and the discharge port is exposed.

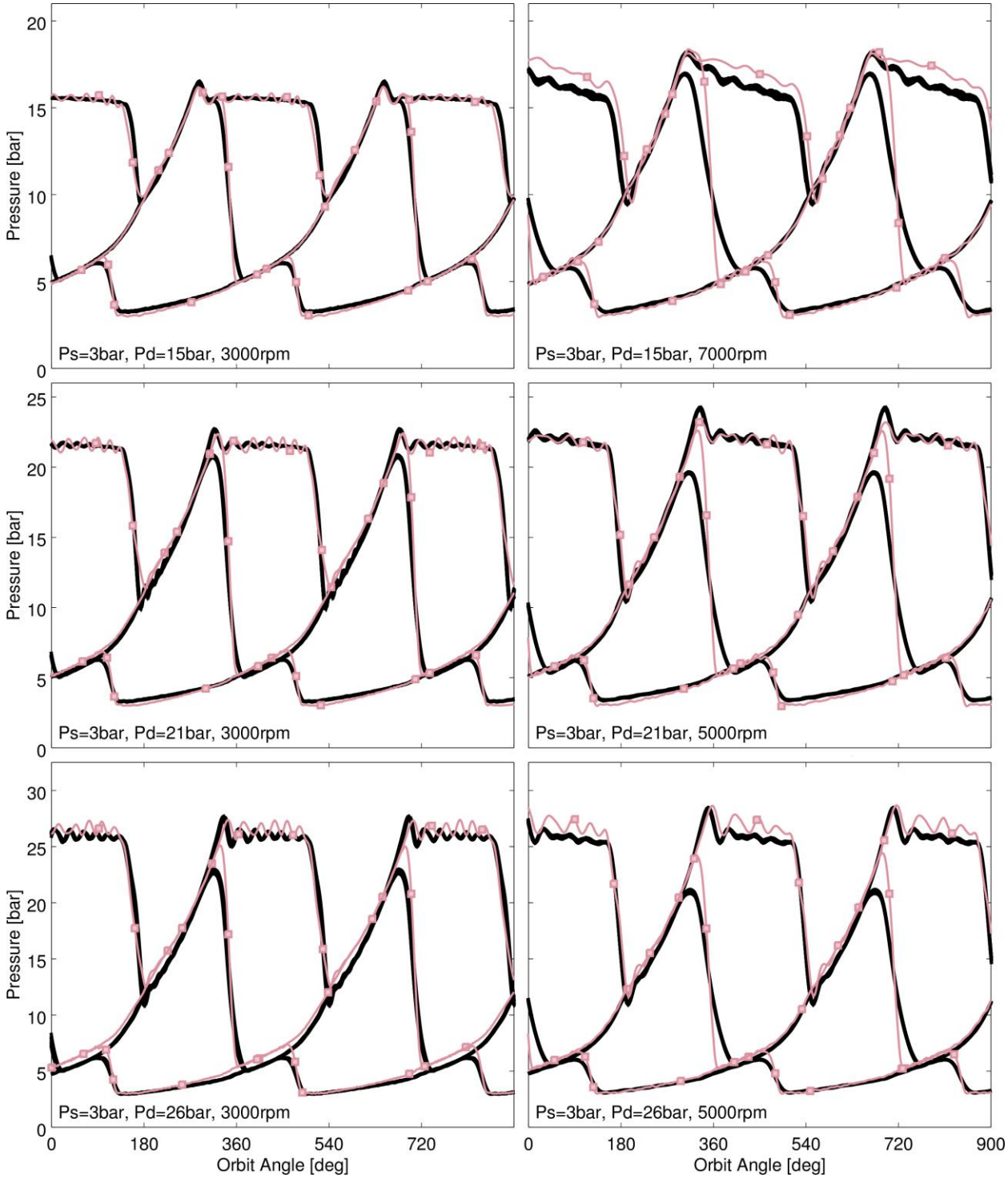

Figure 7: Comparison of internal chamber pressure measurements (black solid lines) and results from the CFD models (rose lines with square markers) for different speeds and discharge pressures.

The quantitative results for the base case models of the various operating conditions are shown first for the chamber pressure measurements in Figure 7. This figure shows the measurements and base case models for six of the operating conditions. Generally, the agreement is satisfactory. In all cases, there is slightly more fluctuation during the discharge process in the model compared to the measurements. At low speed, the magnitude of the pressure at

discharge is very good, but as the speed increases, the model tends to predict a higher pressure than what is measured. Another phenomenon can be observed by the trend with discharge pressure; as the discharge pressure increases, the agreement during the compression phase begins to wane. This is likely due to an under-resolution of the radial leakage flow due to inadequate mesh, or because of neglecting the presence of the lubricating oil in the model. Nevertheless, even at 26 bar, the match during compression is adequate.

Figure 8 shows the pressure pulsation for the 15 bar case compared to the measurements. At high speeds, the general form of the pulsation profile is predicted accurately, although there is slightly more fluctuation in the model. This is amplified at the lower speeds, where the total amplitude is well-predicted, but the high frequency pulsation is more intense. The frequency of the pulsation, however, is well predicted in all of the cases.

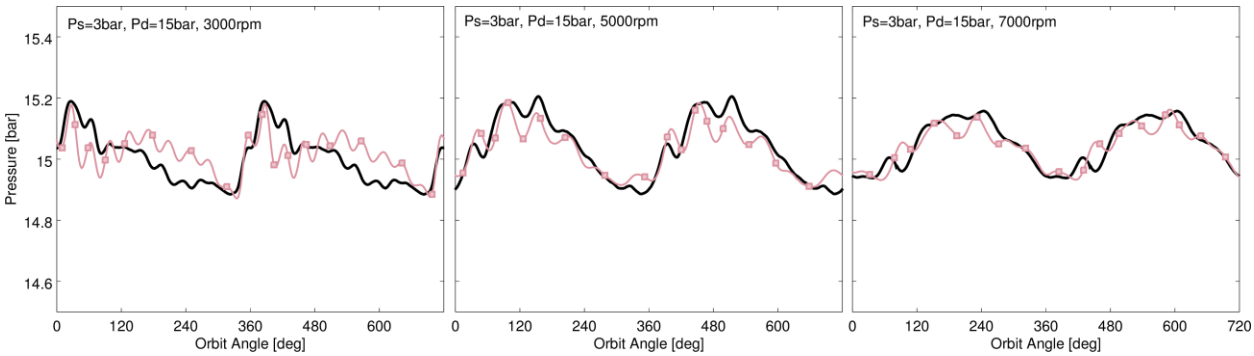

Figure 8: Discharge pressure pulsation from the measurements and CFD model. Colors are the same as Figure 6.

The displacement of the valve is shown in Figure 9 for both the model and measurements. Note that the measurements are only reported when the valve lift exceeds 1.4 mm. As seen in Figure 7, the over-pressure that occurs right before discharge is likely due to the sticking of the reed valve under the forces of the oil surface tension. This had to be accounted for in the model by adding an additional 15 N force to the reed valve when it was closed. This additional force affects the first pressure peak in Figure 7 for each case, and it also affects the opening profile of the reed. With the stiction force added, the reed opens only slightly later, but with larger velocity. The model results were in accord with the measurements, and the calculations with a 15 N stiction force better reproduced the initial opening profile and velocity. As the valve closes, the model tends to under-predict the valve opening, more so at the lower speed. This may also be influenced by the presence of the oil film not accounted for in the model.

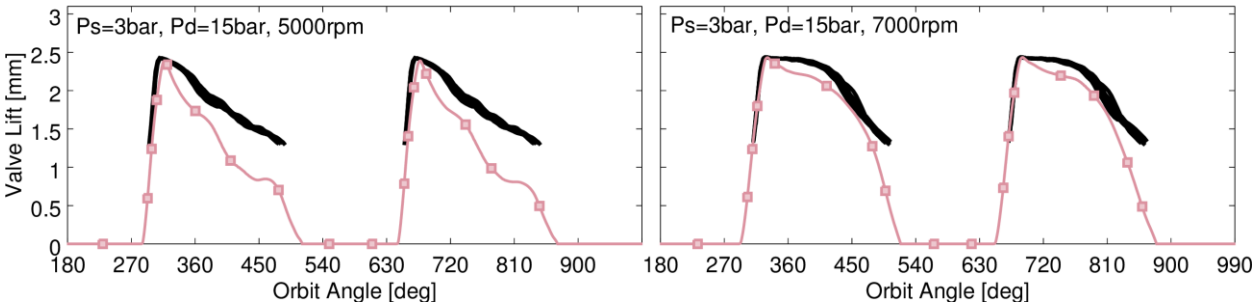

Figure 9: Discharge reed valve lift from the measurements and CFD model. Colors are the same as Figure 6.

In addition to the detailed measurements of the local pressures and valve lift, the global mass flow is an important parameter in determining the compressor's cooling capacity and efficiency. Figure 10 shows the mass flow rate measured both with and without oil present in the compressor and compares to the computed values of the mass flow rate. The maximum deviation is about 8% and occurs at the lowest speed. Two possibilities for the difference include both the over-prediction of the radial leakage flow rate or the over-estimation of the suction preheat temperature entering into the compressor.

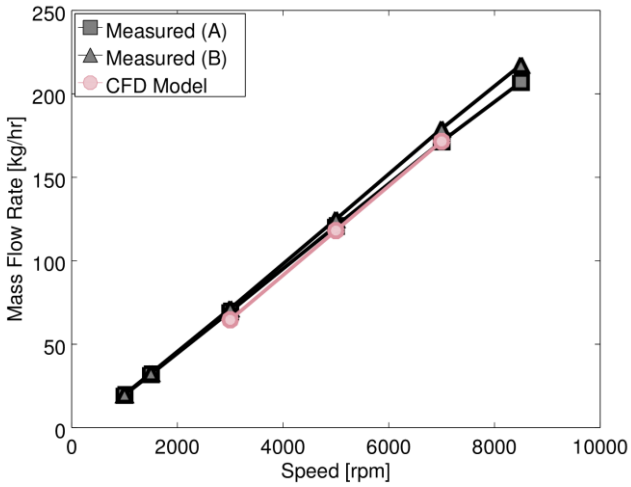

Figure 10: Mass flow rate as a function of orbiting speed for measurements without oil (black squares), measurements with oil (black triangles), and CFD baseline model (rose circles).

4.2 Grid Convergence

In the application of any CFD model it is essential to show that the choice of discretized mesh on which the equations are solved is fine enough to contribute little numerical error compared to the modeling error. In this study, a global grid convergence study is conducted to find out the mesh which results in high enough accuracy and low enough computational cost to be useful in a design optimization context.

All simulations began from the same initial conditions from a mapped coarse run after five cycles and proceeded an additional five cycles. Convergence studies were conducted at two speeds for the 15 bar discharge pressure condition and for one speed each at the two higher discharge pressure conditions. For brevity, only the results of the 5000 rpm case at 15 bar discharge pressure are discussed here, though the conclusions are the similar for the other points.

Figure 11: Planes colored by temperature (top) and velocity (bottom) for two grids in the convergence study. The left is Grid-3, and to the right is Grid-4 as described by Table 2.

The qualitative differences between the grids can be seen in Figure 11, which compares the two finest grids. Due to the use of AMR, the complex velocity patter during discharge is reproduced well even on the coarsest grids. Figure 12 shows more quantitative result comparison for the four grids. Grid 1, the coarsest grid, does exhibit some increased pressure fluctuations. For the prediction of the internal pressure and accurate discharge pressure pulsation amplitude, Grids 3 or 4 should be used. For the accurate reed valve displacement, there is still change on Grid 4, but due to the possibility of missing physics on the oil affect, these modeling errors should be examined first.

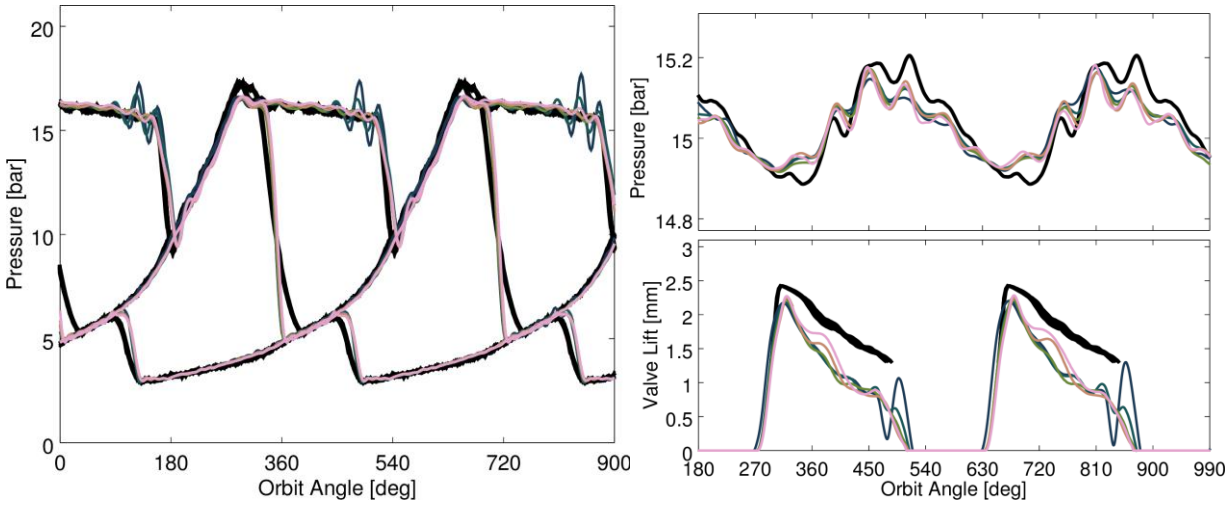

Figure 12: Comparison of measured (black lines) and models with different grid size. The grid sizes corresponding to Table 2 are colored by dark blue (Grid 1), green (Grid 2), orange (Grid 3), and light rose (Grid 4).

Table 1 compares the run time of the different grids over one complete cycle (one rotation of the orbiting scroll). For a typical engineering design cycle Grids 1, 2, and 3 are all reasonably affordable, but if the accuracy required by Grid 4 is required, than increased computing power would be beneficial.

Table 1: Run time information on the four grids studied.

	Base Mesh Size	**Average Cells**	**Run Time**
	[mm]	**[millions]**	**[hr/360deg]**
Grid-1	6.0	0.29	3.0
Grid-2	4.0	0.76	6.3
Grid-3	3.0	1.4	12.8
Grid-4	2.0	3.3	30.6

6. CONCLUSIONS

This work presented the first validation study of a cut-cell based method applied to a scroll compressor with a discharge reed valve. The method has strong advantages for use in engineering design optimization, including the quick transition from CAD geometry to CFD model, ease in making geometry changes, ease of incorporating complex moving boundaries such as the orbiting scroll and the reed valve, low numerical diffusion and high numerical accuracy and stability of the orthogonal cells, and reasonable validation to the experimental compressor measured. The run time for the reasonably accurate results on Grid-3 of 12 hours are low enough for use in engineering purposes, but for design optimization progress should continue in reducing the model cost.

REFERENCES

Bell, I. H., Wronski, J., Quoilin, S., Lemort, V. (2014). Pure and Psuedo-pure Fluid Thermophysical Property Evaluation and the Open-Source Thermophysical Property Library CoolProp. *Industrial & Engineering Chemistry Research*, 53 (6), 2498-2508.

Gao, H., Jiang, Y. (2014). Numerical simulation of unsteady flow in a scroll compressor. Proceedings of the 22nd International Compressor Engineering Conference at Purdue (Paper 2337). West Lafayette, USA: Purdue University.

Hesse, J., Andres R. (2016). CFD simulation of a dry scroll vacuum pump including leakage flows. Proceedings of the 23rd International Compressor Engineering Conference at Purdue (Paper 2498). West Lafayette, USA: Purdue University.

Issa, R. I. (1985). Solution of the Implicitly Discretised Fluid Flow Equations by Operator-Splitting. *Journal of Computational Physics*, 62.

Karypis, G. (2013). A Software Package for Partitioning Unstructured Graphs, Partitioning Meshes and Computing Fill-Reducing Orderings of Sparse Matrices.

Picavet, K., Angel, B. (2016). Numerical simulation of the flow inside a scroll compressor equipped with intermediate discharge valve. Proceedings of the 23rd International Compressor Engineering Conference at Purdue (Paper 2421). West Lafayette, USA: Purdue University.

Pham, H. D., Lehocky, M. (2016). Simulation eines Scroll Verdichter mittels 1D Einsatz, DKV-Tagung 2016, Kassel, Germany.

Pomraning, E., Richards, K., and Senecal, P. (2014). Modeling Turbulent Combustion Using a RANS Model, Detailed Chemistry, and Adaptive Mesh Refinement. *SAE Technical Paper*, #2014-01-1116.

Rhie, C. M. and Chow, W. L. (1983). Numerical Study of the Turbulent Flow Past an Airfoil with Trailing Edge Separation. *AIAA J*., 21, 1525-1532.

Richards, K. J., Senecal, P. K., Pomraning, E. (2017). CONVERGE 2.4 Manual, Convergent Science, Madison, WI.

Rowinski, D. H. and Davis, K. E. (2016). Modeling Reciprocating Compressors using a Cartesian Cut-Cell Method with Automatic Mesh Generation. Proceedings of the 23rd International Compressor Engineering Conference at Purdue (Paper 2511). West Lafayette, USA: Purdue University.

Senecal, P. K., Pomraning, E., Richards, K. J., Briggs, T. E., Choi, C. Y., McDavid, R. M., Patterson, M. A., Hou, S., & Shethaji, T. (2007). A New Parallel Cut-Cell Cartesian CFD Code for Rapid Grid Generation Applied to In-Cylinder Diesel Engine Simulations. *SAE Technical Paper*, #2007-01-0159.

Tillner-Roth, R.; Baehr, H.D. (1994). An international standard formulation of the thermodynamic properties of 1,1,1,2-tetrafluoroethane (HFC-134a) covering temperatures from 170 K to 455 K at pressures up to 70 MPa. *J. Phys. Chem. Ref. Data*, 23, 5, 657-729.

Xiao, G., Liu, G. (2014). Computer simulation for transient flow in oil-free scroll compressor. *International Journal of Control and Automation*, Vol. 7, No. 9, 317-328.

Yakhot, V. and Orszag, S. A. (1986). Renormalization Group Analysis of Turbulence. I. Basic Theory. *J. Sci. Comput.*, 1, 3.